Journal of Structural Geology, Vol. 7, Nos. 3/4, pp. 375 to 383, 1985
Printed in Great Britain

0191-8141/85 $03.00 + 0.00

Implications of a large flattening strain for the origin of a bedding-parallel foliation in the Early Proterozoic Thomson Formation, Minnesota

T. B. HOLST

Department of Geology, University of Minnesota Duluth, Duluth, Minnesota 55812, U.S.A.

(*Received* 7 *February* 1984; *accepted in revised form* 30 *September* 1984)

Abstract—A bedding-parallel foliation exists in an area of multiple deformation in the Early Proterozoic Thomson Formation of Minnesota. Comparison of strain measurements in a region where the bedding-parallel foliation occurs with those from an area where it does not, indicates that a large flattening strain accompanied the development of the foliation. This, and the relationship of the foliation to other structures, demonstrates that it is a tectonic foliation, and not a result of inherited depositional orientation or mimetic recrystallization along bedding.

INTRODUCTION

A FOLIATION parallel or subparallel to bedding is common in the Archean and Proterozoic rocks of the Great Lakes region of North America (e.g. Gruner 1941, Goodwin 1962, Keighin *et al.* 1972, McLimans 1972, Ojakangas 1972, Turner & Walker 1973, Donaldson & Ojakangas 1977, Sawyer 1983), and in poly-deformed terranes in general. The origin and significance of such bedding-parallel foliations have been matters of some discussion. They have been interpreted to be primary depositional fabrics, or an enhancement of a primary fabric by mimetic recrystallization during metamorphism (e.g. Keighin *et al.* 1972, Ojakangas 1972). Alternatively, it has been shown that layer-parallel foliations may form as a result of deformation, which may be quite intense and lead to transposition of bedding (e.g. Davis 1984, p. 442, Hobbs *et al.* 1976, pp. 252–264, Turner & Weiss 1963, pp. 92–95).

A widespread bedding-parallel foliation exists in the southern part of the Early Proterozoic Thomson Formation of Minnesota. It has been suggested that this foliation formed by mimetic recrystallization during a metamorphic event which predated a single deformational event in the region (Keighin *et al.* 1972, Morey 1979). Recently, more than one phase of deformation has been recognized in the area containing the bedding-parallel foliation, the latter having been interpreted to have formed in an early deformational phase (Holst 1982a). This paper presents results of strain measurements in the Thomson Formation which support the interpretation of this foliation as a tectonic fabric.

GEOLOGIC SETTING

The Early Proterozoic Thomson Formation is exposed in east-central Minnesota (Fig. 1), and is thought to be correlative with other rock units of the Animikie Group which overlie the banded iron formations of the Cuyuna, Gunflint, and Mesabi ranges (Morey 1972). The units cannot be directly correlated because of a thick glacial cover. The Thomson Formation is essentially a thick metagreywacke–metasiltstone–slate sequence with minor intercalated graphitic schists, carbonate beds, metavolcanics and rare conglomerates (Morey & Ojakangas 1970, Holst 1984). Details of the sedimentology may be found in Morey & Ojakangas (1970), who concluded that the sequence is a result of turbidity-current deposition. Metamorphic grade in the Thomson Formation varies from lower greenschist facies in the north to lower amphibolite facies (garnet and staurolite zones) in the extreme southernmost outcrops (Morey 1979). The Thomson Formation was deformed and metamorphosed during the Penokean orogeny (1875–1825 Ma, Van Schmus 1976, 1980), a major tectonic event in the Great Lakes region of North America.

STRUCTURAL ZONATION

Northern area

In the northern area of the Thomson Formation (Fig. 1) there are folds with wavelengths from centimeters to kilometers. Most of the folds are open, with some gentle and close folds present and, rarely, tight folds. Fold axial surfaces strike E–W and are vertical or dip steeply to the south. Fold axes trend E–W and are horizontal or plunge a few degrees east or west. Rarely, steep plunges (up to 60°) exist where a fold dies out along trend.

In the northern region there is also a foliation in the rocks which is axial planar to these folds. In the finer-grained units, this is a well-developed continuous slaty cleavage (Fig. 2a). In the units with graded bedding, and in the units with interlaminated fine and coarse layers, the continuous cleavage grades into a disjunctive spaced cleavage (terminology of Powell 1979). The thicker coarse-grained greywacke units also contain a disjunctive spaced cleavage. The spacing of the cleavage domains ranges from continuous up to 1 cm in some of the most coarse-grained units, but it is rarely over a few mm. Cleavage domains constitute from 25% of the rock (in the thick greywacke units) to 100% (in the slates with

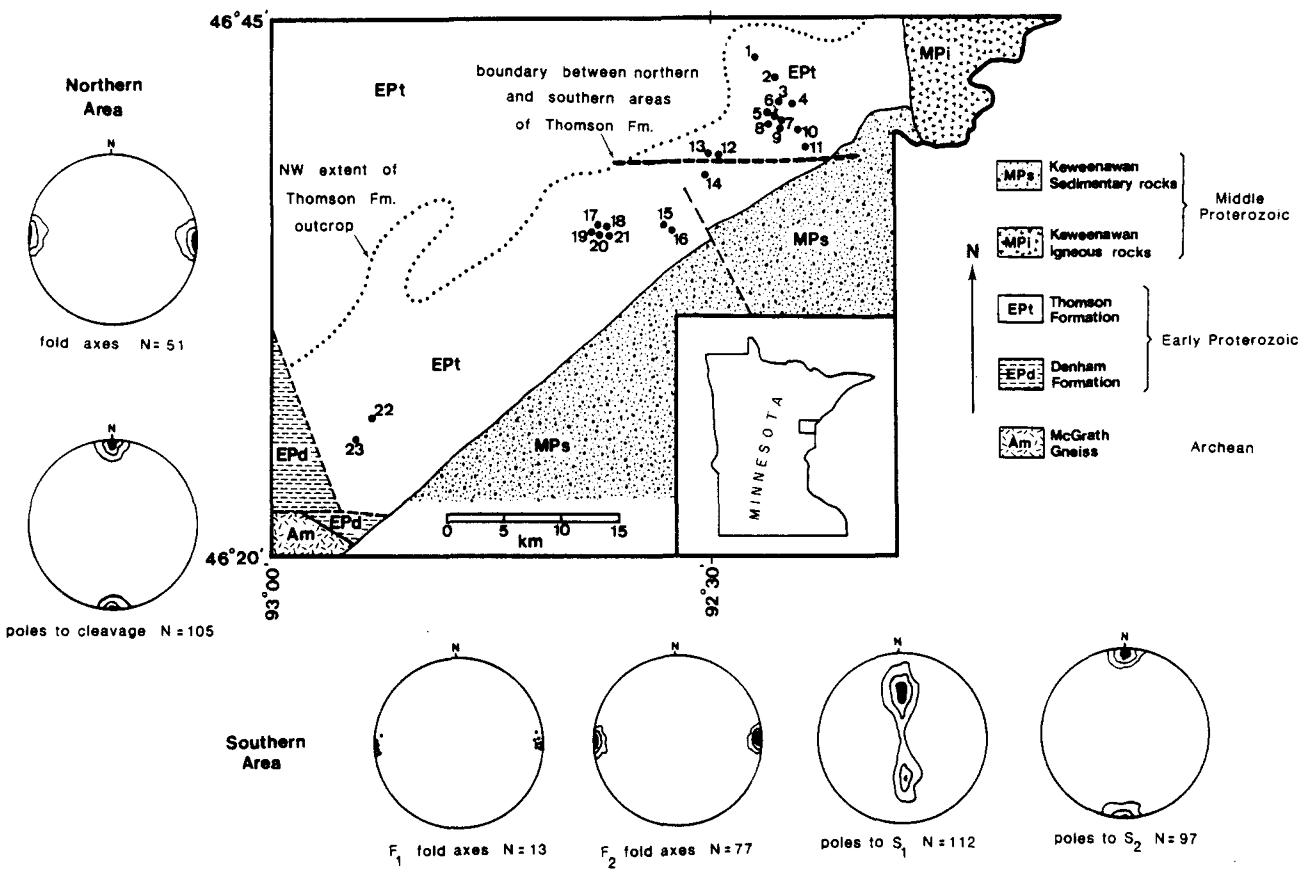

Fig. 1. Generalized geologic map of the area of Thomson Formation exposure (after Morey *et al.* 1981), showing numbered strain-measurement localities. Stereonets to left show orientations of fold axes and cleavage in the northern area. Stereonets at bottom show orientations of F_1 and F_2 axes, and of S_1 and S_2 in the southern area. Contours in each case are 3, 10 and 20% of data per 1% area.

a continuous cleavage). Domain shapes range from rough to smooth (smooth shapes predominate) with some anastomosing shapes. Within the microlithons, a weak fabric, at least, is developed everywhere, and commonly the fabric is strong to complete (Powell 1979).

Southern area

In the southern area (Fig. 1) there is a pervasive foliation (S_1) commonly parallel to bedding in the rock. In the finer-grained beds, this foliation ranges from a fine continuous slaty cleavage in the north, to a schistosity (coarse continuous cleavage or a spaced cleavage with a complete schistose microfabric in microlithons) in the south. In the coarse beds, this foliation is a spaced cleavage with a smooth or slightly rough domainal shape and a strong to complete fabric in the microlithons. Domain spacing is commonly less than 1 mm and cleavage domains constitute from 30 to 100% of the rock.

The S_1 foliation is folded, along with the bedding, into upright, sub-horizontal folds which have the same geometry and orientation as the folds in the northern area. In the southern area, these are F_2 folds.

The bedding-parallel foliation (S_1) is affected by a spaced crenulation cleavage (S_2). This S_2 cleavage can be discrete but is most commonly transitional to zonal, or entirely zonal (Gray 1977, Powell 1979), as illustrated in Figs. 2(b–d). Spacing of the cleavage domains is variable. For the most part, the spaced crenulation cleavage strikes E–W and dips steeply to the south or is vertical, and axial planar to F_2 folds (Fig. 1). However, around some microfolds, the spaced crenulation cleavage may fan, or be at a constant angle (in places up to 40°) to the axial plane on one limb, and axial planar on the other limb. The intersection of S_1 and S_2 defines a well-developed lineation in the rock, trending E–W with sub-horizontal plunges.

F_1 folds are isoclinal and recumbent; fold axes trend within a few degrees of E–W. The S_1 foliation is axial planar to the F_1 folds. Refolding of these isoclinal, recumbent folds by the later upright folds has led to the development of type-3 interference patterns (Ramsay 1967) which can be seen only at outcrop scale (e.g. Holst 1982a, fig. 3), and then only rarely.

Holst (1984) has argued that large-scale fold or thrust nappes developed contemporaneously with the F_1 folds and S_1 foliation in the southern area. The large-scale early structures could also be imbricate thrust fault slices.

STRAIN ANALYSIS

Strain markers in the northern area

The northern area contains a number of outcrops where deformed carbonate concretions may be observed

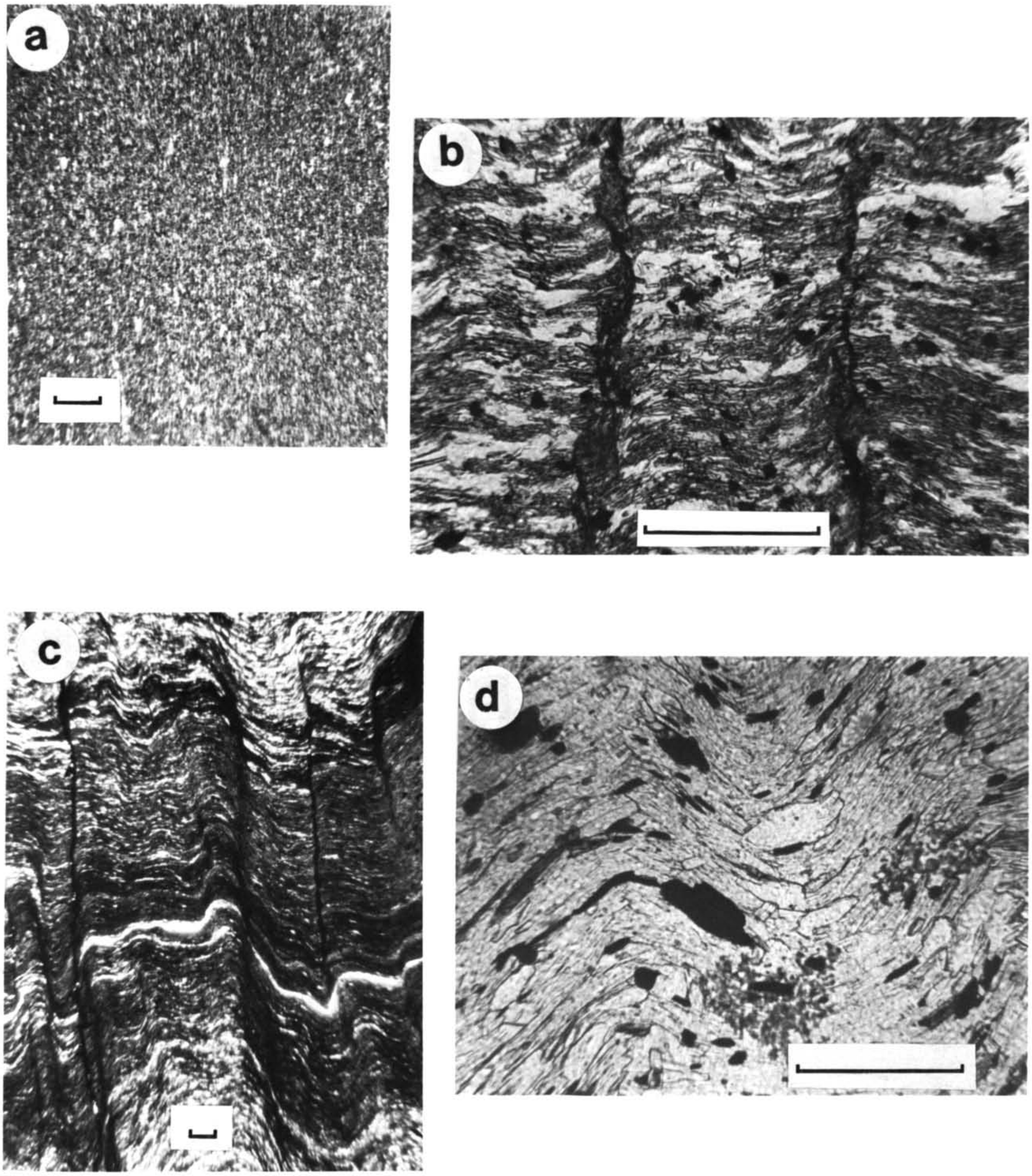

Fig. 2. Photomicrographs showing foliations in the Thomson Formation. All plane-polarized light with 0.25 mm scale bars. (a) Slaty cleavage from northern area. (b–d) S_1 and S_2 from the southern area of Thomson Formation exposure. The S_2 crenulation cleavage runs vertically and S_1 left to right in each case. S_1 is clearly seen to be bedding-parallel in (c).

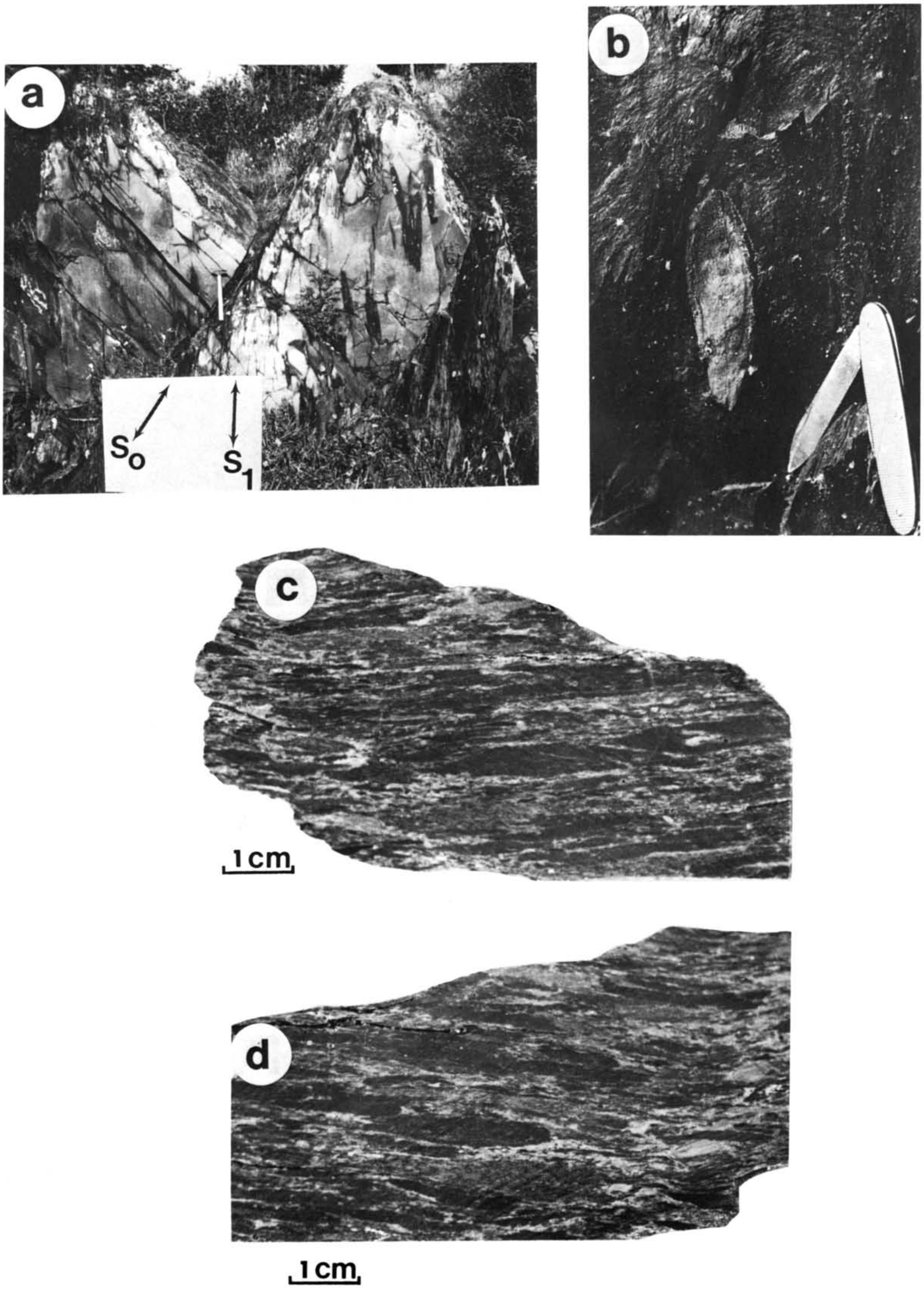

Fig. 3. Strain markers used in the determination of finite strain in the Thomson Formation. (a) Concretions on a N–S vertical joint face, near the type locality. Hammer handle is 40 cm long. S_0 gives bedding orientation, S_1 is the orientation of the only cleavage present in the north. (b) Close-up of concretion, flattened in the cleavage, at locality 10. Knife is 8.5 cm long. (c) and (d) Vertical, mutually perpendicular, sawed sections of conglomerate from locality 20.

(Figs. 3a & b), the origin, composition, and metamorphism of which have been discussed by Schwartz (1942) and Weiblen (1964). The concretions are flattened in the plane of the cleavage and, on a two-dimensional face, their longest dimension ranges from a few centimeters to nearly one meter. These concretions are present in sufficient number on suitable two-dimensional exposure surfaces to allow the measurement of finite strain at several places (Fig. 1). Shape and orientation data were collected from N–S striking vertical joint planes, from cleavage planes (E–W striking and vertical) and from horizontal glaciated outcrop surfaces. Data were also collected from three non-mutually perpendicular planes at locality 1 (Fig. 1).

In addition to flattened concretions, there are at some localities also flattened mud chips present in sufficient number for strain analysis (localities 8, 12 and 13, Fig. 1). At locality 4 (Fig. 1) a thin deformed conglomerate bed was also used to measure strain. At the 13 strain-measurement localities in the northern area, bedding was at a variety of dips, and small-scale folds were present at several localities.

Strain markers in the southern area

In the southern area there are several places where mud chips are present and exposure is sufficient for strain data to be collected (localities 14, 15, 16, 22 and 23, Fig. 1). A number of strain determinations were also done using deformed conglomerate pebbles (localities 17–21, Fig. 1). The pebbles are of a variety of clastic rock types, which range from slates to metagreywackes with finer-grained fragments predominant (Figs. 3c & d). At all 10 strain-measurement localities in the southern area, bedding and S_1 were subhorizontal, and lay at or near the hinge of F_2 folds.

Two-dimensional strain analysis

At the locations where concretions or mud chips were used as strain markers, two-dimensional finite-strain states were calculated using shape and orientation data gathered in the field from the deformed markers. An attempt was made to measure shape ratio and orientation of 100 deformed objects on each face used. In some places this was not possible, and data from parallel outcrop faces, located within a few meters of each other, were combined. The most difficult data to collect were from cleavage faces (in the north), and less than 100 deformed objects were measured; the lowest number of deformed objects measured on any face that was used in strain analysis was 35.

Oriented samples of the conglomerates were collected in the field, and cut on three mutually perpendicular faces. Two-dimensional strain analyses were carried out on these faces by measuring shapes and orientations of the deformed clasts, and also using the clast-centers technique given by Fry (1979) for some faces.

For the mud chips and the conglomerate clasts, the problem of competence contrast between the deformed object and the matrix is negligible as matrix and objects are essentially the same composition. This is not readily apparent for the carbonate concentrations. However, strains calculated separately using mud chips and concretions, where both were available at a station, were in good agreement indicating the competence contrast between the carbonate concretions and the host rock was similar to that of the mud chips, and probably small.

The shape and orientation data were plotted using the polar plot of Elliott (1970) and on standard ln $R_f - \phi$ plots (Ramsay 1967, Dunnet & Siddans 1971). Strain was calculated using the method of Holst (1982b) for determining the initially circular point on the polar plot.

Results for deformed concretions on one of the non-cleavage faces at locality 10 are shown in Fig. 4. Nearly all the long axes of the deformed concretions lie along the cleavage trace on this face. This is true for both mud chips and concretions on all non-cleavage faces in the northern area (localities 1–13). The degree to which the mud chips and concretions are flattened in the plane of the cleavage is striking. This low fluctuation (Cloos 1947) indicates that prior to deformation the mud chips and concretions had rather low shape ratios. For locality 10, the R_i contours of Fig. 4(a) show that this initial shape factor was less 1.5 : 1 for nearly all particles, and quite a bit less than 1.5 : 1 for most.

The clasts in the conglomerates show a greater range in shape and orientation in the deformed state (Fig. 5), reflecting a greater range in initial shape and orientation. Strains calculated using shape and orientation data are in good agreement with Fry's (1979) method for the conglomerates (e.g. Fig. 5).

Three-dimensional strain analysis

Three-dimensional strain ellipsoids were calculated using the two-dimensional data from three mutually perpendicular planes. For locality 1, where the planes for which available two-dimensional data were not mutually perpendicular, the technique of Ramsay (1967, p. 147) was used. For the sawed samples of conglomerate, the three planes were not the principal planes. For the measurements taken directly from field exposure, the three planes turn out to be the principal planes.

The shapes of the strain ellipsoids are shown in Fig. 6, and calculated strain parameters are listed in Table 1. The strains in the northern area of the Thomson Formation plot in a relatively small region of the flattening field ($0 < K < 1$). The strains in the southern region also plot in a small area with all but locality 21 falling just into the constrictional field ($1 < K < \infty$). Values of the parameter r are consistent within each area (Table 1) with slightly higher values in the south (average of $r = 6.5$) than in the north (average of $r = 5.2$).

The orientations of the principal extensions are shown in Fig. 7. In the north, the greatest principal extension (X) is vertical, Y is horizontal and trends E–W (parallel to the fold axes), and Z trends N–S and is horizontal. In the south, X is horizontal and trends E–W (parallel to F_1 and F_2 fold axes), Y is horizontal and trends N–S and Z is vertical.

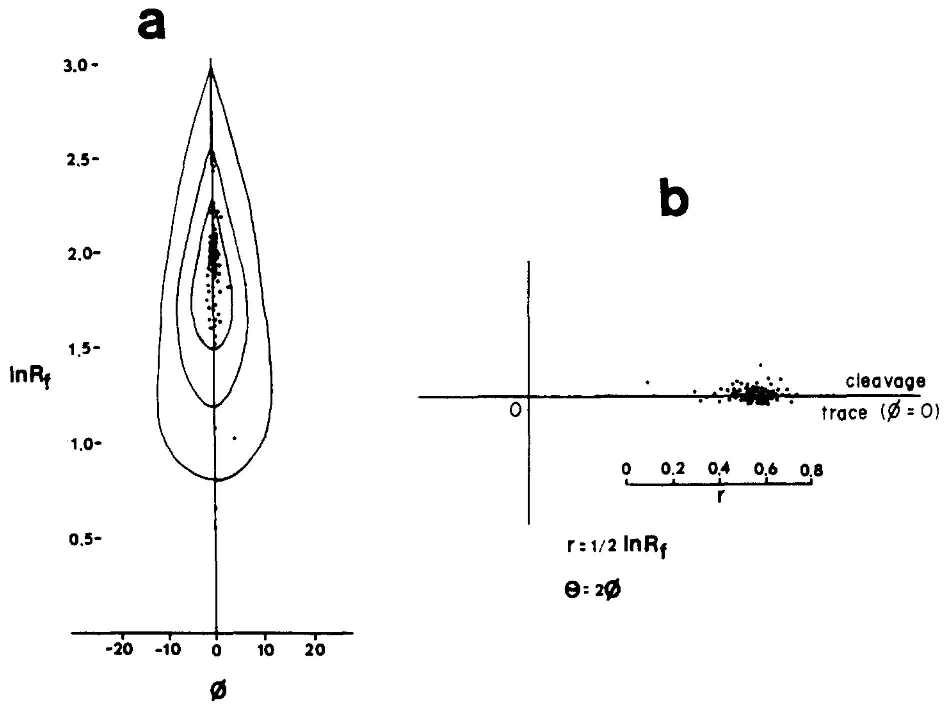

Fig. 4. Two-dimensional strain determination results from a N–S vertical joint face at locality 10. (a) ln R_f vs ϕ plot. Contours are for R_i values of 1.5, 2.0 and 3.0 for a strain of 6.7 : 1. (b) Same data on the polar plot. Scale is radius vector ($r = \frac{1}{2}\ln R_f$); $\theta = 2\phi$. Reference line ($\phi = 0$) is the cleavage trace on the face.

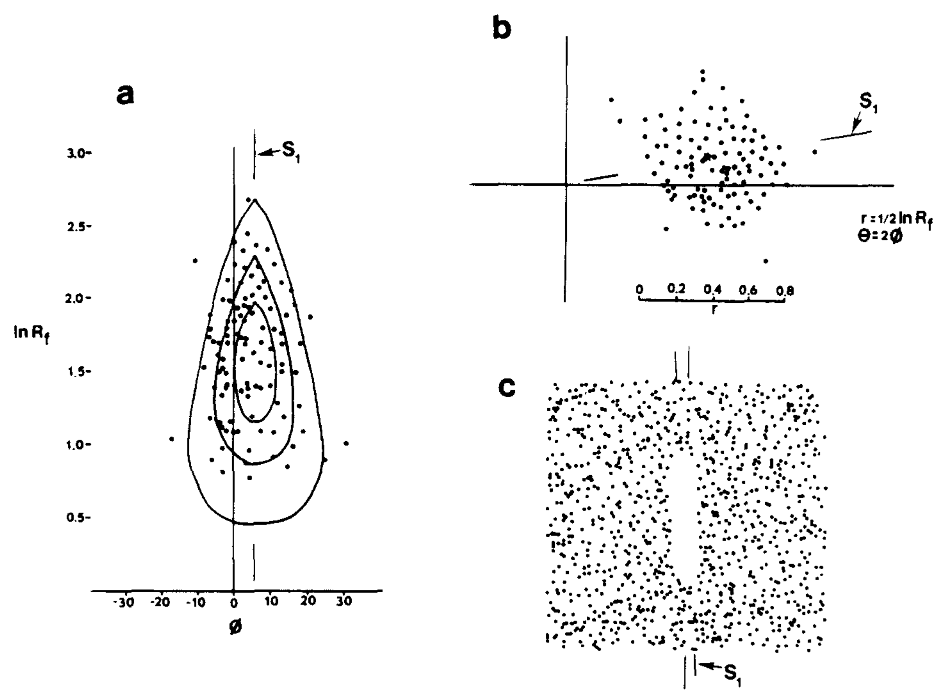

Fig. 5. Two-dimensional strain determination results from a saw-cut vertical face of a deformed conglomerate at locality 20. (a) ln R_f vs ϕ plot, contours are for R_i values of 1.5, 2.0, and 3.0 for a strain of 4.7 : 1; $\phi = 6°$. (b) Same data on the polar plot, scale is radius vector $\theta = 2\phi$. Star is initially circular point from the method of Holst (1982b). Strain is 4.7 : 1; $\phi = 6°$. (c) Results for same face with the center method of Fry (1979). Strain is 4.8 : 1; $\phi = 6°$. In each of the diagrams, S_1 shows the trace of the bedding-parallel foliation on the face. $\phi = 0$ is reference line on rock face.

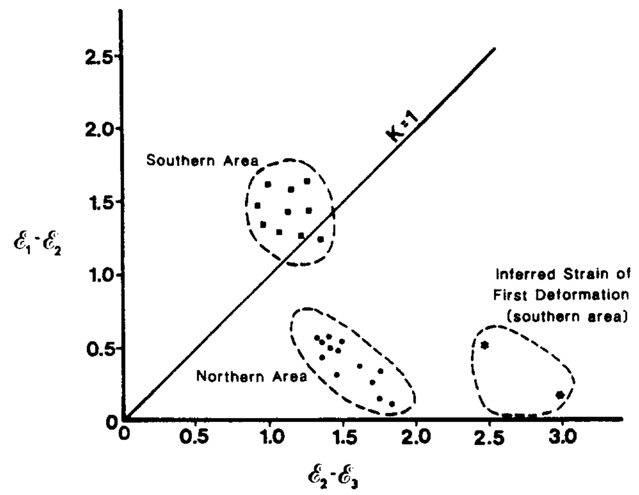

Fig. 6. Logarithmic deformation plot showing results of three-dimensional strain analyses. Stars represent inferred finite strains associated with the first deformation of the southern area (see text). Dashed lines surround areas showing the strain of the first deformation (stars), the second deformation (dots) and the total strain in the area of multiple deformation (boxes).

DISCUSSION

Northern area strain

In the northern area, where the slaty cleavage is the only foliation present, the strain ellipsoids plot in the center of the field defined by Wood's 5200 strain determinations in slates (Wood 1974, fig. 4). Wood found the maximum extension (X) was most commonly vertical (sub-orthogonal to fold axes) and this is also true for the northern area of the Thomson Formation. Additionally, the mean calculated shortening perpendicular to slaty cleavage in the northern area is 64%, in good agreement with Wood's results.

No meaningful pattern of strain variation was found in the northern area. Strain orientation is consistent over the region (Fig. 7) and there is no consistent increase or decrease in strain in any direction; there is as much variation in strain between two closely spaced localities as there is across the area (Fig. 1, Table 1). The con-

Table 1. Calculated three-dimensional strain parameters

Locality	a	b	$\varepsilon_1 - \varepsilon_2$	$\varepsilon_2 - \varepsilon_3$	k	K	r
Northern area							
1	1.55	3.92	0.44	1.37	0.19	0.32	4.47
2	1.39	5.84	0.33	1.76	0.08	0.19	6.23
3	1.62	4.35	0.48	1.47	0.19	0.33	4.97
4	1.11	6.12	0.10	1.81	0.02	0.06	6.23
5	1.31	5.47	0.27	1.70	0.07	0.16	5.78
6	1.89	4.42	0.64	1.49	0.26	0.43	5.31
7	1.80	4.06	0.59	1.40	0.26	0.42	4.86
8	1.65	4.11	0.50	1.41	0.21	0.35	4.76
9	1.79	3.74	0.58	1.32	0.29	0.44	4.53
10	1.75	3.86	0.56	1.35	0.26	0.41	4.61
11	1.47	5.01	0.39	1.61	0.12	0.24	5.48
12	1.36	4.35	0.31	1.47	0.11	0.21	4.71
13	1.15	5.83	0.14	1.76	0.03	0.08	5.98
Southern area							
14	3.65	2.92	1.30	1.07	1.38	1.15	5.57
15	4.23	3.92	1.44	1.37	1.11	1.05	7.15
16	4.89	3.74	1.59	1.32	1.42	1.20	7.63
17	3.75	3.42	1.32	1.23	1.14	1.07	6.17
18	3.80	2.61	1.34	0.96	1.74	1.39	5.41
19	5.09	3.52	1.63	1.26	1.62	1.29	7.61
20	4.18	3.19	1.43	1.16	1.45	1.23	6.37
21	3.41	3.85	1.23	1.35	0.85	0.91	6.26
22	4.36	2.51	1.48	0.92	2.23	1.60	5.87
23	5.00	2.65	1.61	0.97	2.42	1.65	6.65

Numbered localities shown on Fig. 1. $a = X/Y$; $b = Y/Z$; $X > Y > Z$ (Flinn 1962). $\varepsilon_1 - \varepsilon_2 = \ln a$; $\varepsilon_2 - \varepsilon_3 = \ln b$ (Ramsay 1967, p. 329). $k = (a-1)/(b-1)$ (Flinn 1962). $K = (\ln a)/(\ln b)$ (Ramsay 1967, p. 329). $r = a + b - 1$ (Watterson 1968).

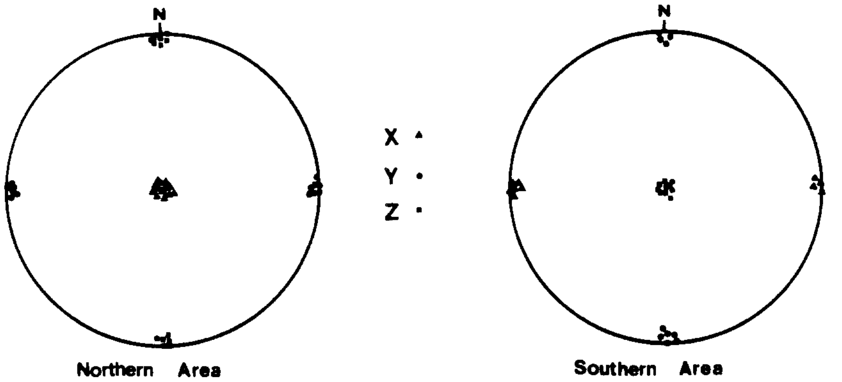

Fig. 7. Orientations of X, Y & Z ($X > Y > Z$) shown on Schmidt nets from the 13 strain localities in the northern area and the 10 localities in the southern area.

sistency of strain-marker shape around a fold also indicates homogeneity of strain with respect to folds. Thus, the strain in the northern area is basically that of the center of the area marked on Fig. 6, with differences in measured strain caused by local strain variations and uncertainties in the strain-measurement techniques.

Southern area strain

The results of strain-measurements in the southern area give quite consistent orientations, shapes, and magnitudes across the whole region (Figs. 1, 6 and 7; Table 1). Again, no consistent strain variation or pattern is seen, and there is as much strain variation in very closely spaced localities as there is across the area (Figs. 1 and 6, Table 1). This consistency may be, to a degree, a result of the relative paucity of suitable strain markers in the southern region (localities 15 & 16 are within a few tens of meters of each other, as are localities 17–21) and the fact that all strain localities in the south are at or near hinges of F_2 folds where strain histories may have been less complex.

An important difference from the northern area, however, is the orientation of the XY plane of strain. On average, it is horizontal (actually subhorizontal at F_2 fold hinges) and lies parallel to bedding and to the early bedding-parallel foliation. This is in spite of the fact that some shortening must have taken place in a N–S direction, parallel to bedding, during the later development of crenulation cleavage and upright F_2 folds. Thus, the measured strains of the southern area are total strains resulting from the superposition of two deformation phases. Furthermore, the earlier of these two phases would have had a greater extension in the N–S direction than that which is shown by the total strain.

Although it is not possible to determine precisely the magnitude of these two strain episodes from the available data, order of magnitude values can be estimated if some assumptions are made. The geometry and orientation of F_2 folds and the S_2 crenulation cleavage in the south are identical to the folds and slaty cleavage in the north. Radiometric age determinations (both K/Ar and Rb/Sr) of the latest metamorphism give consistent results from north to south throughout the Thomson Formation (Goldich *et al.* 1961, Peterman 1966, Keighin *et al.* 1972). Thus, the strain of the second deformation in the south may also be similar in magnitude and orientation to the measured strain in the northern area. Given the consistency of strain measurement results in both northern and southern areas, strain ellipsoids from the center of the areas marked on Fig. 6 were chosen as representative for each area (Fig. 8, top two block diagrams). As these are coaxial, it is a simple matter to remove the strain of the second deformation (northern area strain, top left block, Fig. 8) from the total cumulative strain measured in the south (top right block, Fig. 8). The resultant strain ellipsoid for the first deformation in the south is of the extreme flattening type. This is plotted as a star in the lower right-hand corner of Fig. 6, and is illustrated as block diagram Model I in the lower

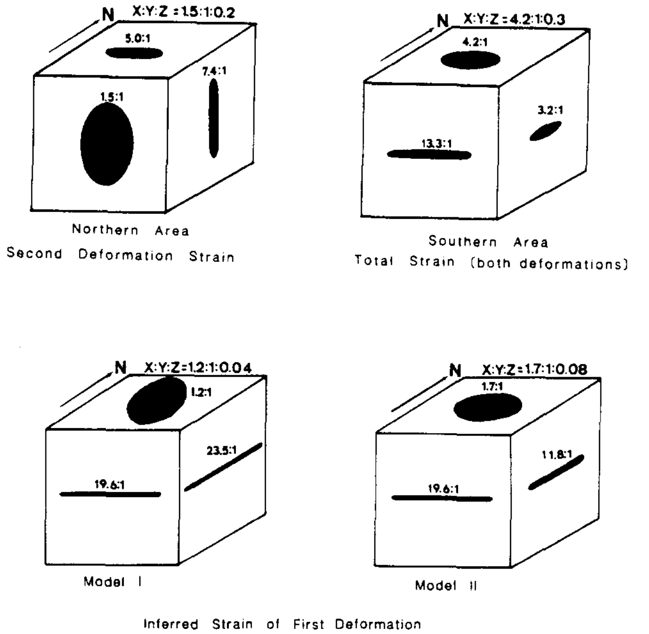

Fig. 8. Representative block diagrams of the state of finite strain in the northern and southern areas, and the strain inferred to have been associated with the first deformation. See text for details.

left-hand corner of Fig. 8. Z in this model is vertical, and X is horizontal and trends N–S, orthogonal to F_1 fold axes. This model indicates a large amount of extension within the plane of the S_1 foliation, and there are abundant examples of boudinage (in all directions) within the plane of the S_1 foliation in the southern area (Holst 1982a).

Other models are also possible. The second-deformation shortening in the south may not have been as great as in the north, as the rocks in the south had a previous foliation. A second estimate of strain associated with the first deformation in the south was made, with assumptions as before, but with half as much shortening in the second deformation. The resultant strain ellipsoid is the upper left star in Fig. 6, and the lower right block diagram (Model II) in Fig. 8. This is, again, a high flattening strain, with Z vertical, and X horizontal. But the maximum extension direction, X, now lies E–W, parallel to F_1 fold axes, instead of N–S.

Whatever the model or the assumptions used, a large flattening strain must have accompanied the development of the S_1 bedding-parallel foliation, with high values of shortening perpendicular to the foliation. Such a large strain, and particularly one showing such a large extension, is unlikely to have been caused by compaction or primary effects. It could only have resulted from a tectonic deformation. Thus, the bedding-parallel foliation with which it is associated is not primary, or just the result of a mimetic recrystallization, but is a tectonic foliation. This is in agreement with previous structural observations (Holst 1982a, 1984) which point to a major recumbent folding episode in the southern area in early Penokean time.

Acknowledgements—Jeff Feenstra aided in the collection of clast shape and orientation data. Dick Clark, Mark Connolly and Peter

McSwiggen helped locate outcrops suitable for strain analysis. The author gratefully acknowledges helpful discussions with Dave Gray, Gautam Mitra, and Chris Powell and the comments of Jean-Pierre Burg and David Durney in review. This research was supported by National Science Foundation Grant EAR8120951.

REFERENCES

Cloos, E. 1947. Oolite deformation in the South Mountain fold, Maryland. *Bull. geol. Soc. Am.* **58**, 843–918.

Davis, G. H. 1984. *Structural Geology of Rocks and Regions.* Wiley, New York.

Donaldson, J. A. & Ojakangas, R. W. 1977. Orthoquartzite pebbles in Archean conglomerate, North Spirit Lake, northwestern Ontario. *Can. J. Earth Sci.* **14**, 1980–1990.

Dunnet, D. & Siddans, A. W. B. 1971. Non-random sedimentary fabrics and their modification by strain. *Tectonophysics* **12**, 307–325.

Elliott, D. 1970. Determination of finite strain and initial shape from deformed elliptical objects. *Bull. geol. Soc. Am.* **81**, 2221–2236.

Flinn, D. 1962. On folding during three dimensional progressive deformation. *Q. Jl geol. Soc. Lond.* **118**, 385–433.

Fry, N. 1979. Random point distributions and strain measurement in rocks. *Tectonophysics* **60**, 89–105.

Goldich, S. S., Nier, A. O., Baadsgaard, H., Hoffman, J. H. & Krueger, H. W. 1961. The Precambrian geology and geochronology of Minnesota. *Bull. Minn. geol. Surv.* **41**, 1–193.

Goodwin, A. M. 1962. Structure, stratigraphy, and origin of iron-formation, Michipicoten area, Algoma district, Ontario. *Bull. geol. Soc. Am.* **73**, 561–586.

Gray, D. R. 1977. Morphologic classification of crenulation cleavages. *J. Geol.* **85**, 229–235.

Gruner, J. W. 1941. Structural geology of the Knife Lake Area of Northeastern Minnesota. *Bull. geol. Soc. Am.* **52**, 1577–1642.

Hobbs, B. E., Means, W. D. & Williams, P. F. 1976. *An Outline of Structural Geology.* Wiley, New York.

Holst, T. B. 1982a. Evidence for multiple deformation during the Penokean Orogeny in the Middle Precambrian Thomson Formation, Minnesota. *Can. J. Earth Sci.* **19**, 2043–2047.

Holst, T. B. 1982b. The role of initial fabric on strain determination from deformed ellipsoidal objects. *Tectonophysics* **82**, 329–350.

Holst, T. B. 1984. Evidence for nappe development during the Early Proterozoic Penokean Orogeny, Minnesota. *Geology* **12**, 135–138.

Keighin, C. W., Morey, G. B. & Goldich, S. S. 1972. East-central Minnesota. In: *Geology of Minnesota: A Centennial Volume* (edited by Sims, P. K. & Morey, G. B.). *Minn. geol. Surv.*, Saint Paul, Minnesota, 240–255.

McLimans, R. K. 1972. Granite-bearing conglomerates in the Knife Lake Group, Vermilion District. In: *Geology of Minnesota: A Centennial Volume* (edited by Sims, P. K. & Morey, G. B.). *Minn. geol. Surv.*, Saint Paul, Minnesota, 91–97.

Morey, G. B. 1972. Middle Precambrian general geologic setting. In: *Geology of Minnesota: A Centennial Volume* (edited by Sims, P. K. & Morey, G. B.). *Minn. geol. Surv.*, Saint Paul, Minnesota, 199–203.

Morey, G. B. 1979. Stratigraphic and tectonic history of east-central Minnesota. In: *Field Trip Guidebook for Stratigraphy, Structure, and Mineral Resources of East-Central Minnesota* (edited by Balaban, N. H.). Institute on Lake Superior Geology and North-central Section, *Geol. Soc. Am.*, Annual Meetings, Duluth, Minnesota, 13–28.

Morey, G. B. & Ojakangas, R. W. 1970. Sedimentology of the middle Precambrian Thomson Formation, east-central Minnesota. *Minn. geol. Surv. Rep. Invest.* **13**, Saint Paul, Minnesota, 1-32.

Morey, G. B., Olsen, B. M. & Southwick, D. L. 1981. *Geologic Map of East-Central Minnesota at* 1:250,000. *Minn. geol. Surv.*, Saint Paul, Minnesota.

Ojakangas, R. W. 1972. Rainy Lake Area. In: *Geology of Minnesota: A Centennial Volume* (edited by Sims, P. K. & Morey, G. B.). *Minn. geol. Surv.*, Saint Paul, Minnesota, 163–171.

Peterman, Z. E. 1966. Rb–Sr dating of middle Precambrian metasedimentary rocks of Minnesota. *Bull. geol. Soc. Am.* **77**, 1031–1044.

Powell, C. McA. 1979. A morphological classification of rock cleavage. *Tectonophysics* **58**, 21–34.

Ramsay, J. G. 1967. *Folding and Fracturing of Rocks.* McGraw-Hill, New York.

Sawyer, E. W. 1983. The structural history of a part of the Archean Quetico metasedimentary belt, Superior province, Canada. *Precambrian Res.* **22**, 271–294.

Schwartz, G. M. 1942. Concretions of the Thomson Formation, Minnesota. *Am. J. Sci.* **240**, 491–499.

Turner, C. C. & Walker, R. G. 1973. Sedimentology, stratigraphy and crustal evolution of the Archean greenstone belt near Sioux Lookout, Ontario. *Can. J. Earth Sci.* **10**, 817–845.

Turner, F. J. & Weiss, L. E. 1963. *Structural Analysis of Metamorphic Tectonites.* McGraw-Hill, New York.

Van Schmus, W. R. 1976. Early and middle Proterozoic history of the Great Lakes area, North America. *Phil. Trans. R. Soc.* **A280**, 605–628.

Van Schmus, W. R. 1980. Chronology of igneous rocks associated with the Penokean orogeny in Wisconsin. In: *Selected Studies of Archean Gneisses and Lower Proterozoic Rocks, Southern Canadian Shield* (edited by Morey, G. B. & Hanson, G. N.). *Spec. Pap. geol. Soc. Am.* **182**, 159–168.

Watterson, J. 1968. Homogeneous deformation of the gneisses of Vesterland, southwest Greenland. *Meddr. Grønland* **175**, 1–75.

Weiblen, P. W. 1964. A preliminary study of the metamorphism of the Thomson Formation. Unpublished M.S. thesis, University of Minnesota, Minneapolis.

Wood, D. S. 1974. Current views of the development of slaty cleavage. *A. Rev. Earth Planet. Sci.* **2**, 1–35.